Ferroelectric Liquid Crystals Induced by Atropisomeric Dopants: Dependence of the Polarization Power on the Core Structure of the Smectic C Host

Despina Vizitiu, Carmen Lazar, Brian J. Halden, and Robert P. Lemieux*

Contribution from the Department of Chemistry, Queen's University, Kingston, Ontario, Canada K7L 3N6

Received March 24, 1999. Revised Manuscript Received July 1, 1999

Abstract: A series of 11 chiral dopants with an atropisomeric core derived from 4,4′-dihydroxy-2,2′,6,6′-tetramethyl-3,3′-dinitrobiphenyl were synthesized in optically pure form. These compounds were doped into five different smectic C (S_C) liquid crystal hosts to induce a ferroelectric S_C* liquid crystal phase, and the reduced polarization P_o was measured as a function of the dopant mole fraction x_d over the range $0.005 < x_d \leq 0.05$. The polarization power δ_p was found to strongly depend on the core structure of the S_C host. For example, the dopant (+)-2,2′,6,6′-tetramethyl-3,3′-dinitro-4,4′-bis[(4-octyloxybenzoyl)oxy]biphenyl gave δ_p values of <30 nC/cm^2 in a phenyl benzoate S_C host and 1738 nC/cm^2 in a phenylpyrimidine S_C host; the latter is one of the highest polarization power values reported thus far in the literature. In the phenylpyrimidine S_C host, the polarization power was found to depend on the length of the dopant side chains and on the position of the atropisomeric core with respect to those of the surrounding S_C host molecules, on the time average. The polarization power followed a trend opposite to that followed by the S_C* helical pitch. Analysis of these results suggests that chirality transfer from the atropisomeric core of the dopant to those of the S_C host molecules plays a key role in amplifying the polarization induced in the phenylpyrimidine host. It is likely that such intercore chirality transfer results in an asymmetric distortion of the S_C* lattice, which in turn, further increases the conformational asymmetry of the chiral dopant by virtue of increased diastereomeric bias between the S_C* lattice and the chiral conformations of the dopant.

Introduction

A chiral smectic C (S_C*) liquid crystal phase, which is ferroelectric as a surface-stabilized thin film (vide infra), can be obtained by doping an achiral smectic C (S_C) liquid crystal host with a chiral additive that may or may not be mesogenic.[1] On the time average, the symmetry elements of an achiral smectic C (S_C) liquid crystal phase include a C_2 axis normal to the tilt plane (defined by the molecular long axis **n** and the layer normal **z**) and a reflection plane of symmetry σ congruent with the tilt plane, as shown in Figure 1. The introduction of a chiral dopant into a S_C liquid crystal breaks the reflection symmetry and results in the polar ordering of transverse molecular dipoles along the C_2 axis, which is now a *polar axis*, thus resulting in a net spontaneous polarization (P_S).[2] In the absence of external constraints, however, a chiral S_C* liquid crystal forms a macroscopic helical structure in which the spontaneous polarization rotates from one layer to the next, thus averaging to zero in the bulk.

Clark and Lagerwall have shown that the helical structure of a S_C* liquid crystal spontaneously unwinds between polyimide-coated glass slides with a spacing of 1−5 μm to give a surface-stabilized ferroelectric liquid crystal (SSFLC) with a net spontaneous polarization along the polar C_2 axis, which is perpendicular to the glass slides.[3] By applying an electric field

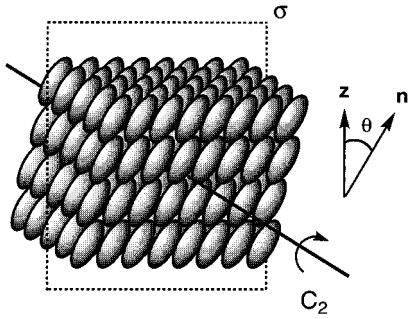

Figure 1. Schematic representation of the smectic C phase. The vectors **z** and **n** are in the plane of the page.

E across the glass slides, a SSFLC can be switched between two degenerate surface-stabilized states corresponding to opposite tilt orientations, thus producing a change in birefringence when the SSFLC film is placed between crossed polarizers. This effect is now being exploited in high-resolution display applications.[4] The switching time (τ_s) of a SSFLC light valve is a function of P_S, the orientational viscosity (η), and the applied field (E) according to eq 1.[4c] Because S_C* mesogens with high P_S tend to have high orientational viscosities, commercial S_C* mixtures suitable for SSFLC display applications are normally

* To whom correspondence should be addressed. E-mail: lemieux@chem.queensu.ca.

(1) Kuczynski, W.; Stegemeyer, H. *Chem. Phys. Lett.* **1980**, *70*, 123.

(2) Meyer, R. B.; Liebert, L.; Strzelecki, L.; Keller, P. *J. Phys. (Paris) Lett.* **1975**, *36*, L69.

(3) Clark, N. A.; Lagerwall, S. T. *Appl. Phys. Lett.* **1980**, *36*, 899.

(4) (a) Lagerwall, S. T. In *Handbook of Liquid Crystals*; Demus, D., Goodby, J. W., Gray, G. W., Spiess, H. W., Vill, V., Ed.; Wiley-VCH: Weinheim, 1998; Vol. 2B. (b) Walba, D. M. *Science* **1995**, *270*, 250. (c) Goodby, J. W.; Blinc, R.; Clark, N. A.; Lagerwall, S. T.; Osipov, M. A.; Pikin, S. A.; Sakurai, T.; Yoshino, K.; Zeks, B. *Ferroelectric Liquid Crystals: Principles, Properties and Applications*; Gordon & Breach: Philadelphia, 1991. (d) Dijon, J. In *Liquid Crystals: Applications and Uses*; Bahadur, B., Ed.; World Scientific: Singapore, 1990; Vol. 1, Chapter 13.

10.1021/ja990965m CCC: $18.00
Published on Web 08/31/1999

obtained by mixing a chiral dopant with a propensity to induce high P_S into an achiral S_C liquid crystal mixture with a low viscosity and a wide temperature range.

$$\tau_s \propto \eta/P_S E \tag{1}$$

The spontaneous polarization and tilt angle (θ) of a S_C* phase are related by eq 2 to the reduced polarization (P_o), which is intrinsic to the chiral component of the S_C* liquid crystal at a fixed temperature difference below the S_C*−S_A* or S_C*−N* phase transition ($T - T_C$).[1] The propensity of a chiral dopant to induce a spontaneous polarization in a S_C host can be expressed as the polarization power (δ_p) according to eq 3, in which x_d is the dopant mole fraction.[5] This relationship is generally found to be linear when $x_d < 0.1$. It is now well established that the magnitude and sign of P_o in induced S_C* liquid crystals depend on the molecular structure and absolute configuration of the chiral dopant, respectively.[6,7] More recently, studies have shown that, for certain types of chiral dopants, the induced polarization can also depend on the nature of the S_C host.[8] To rationally design chiral dopants with high δ_p—and achieve fast switching in SSFLC display applications—a detailed understanding of these structure−property relationships must be achieved.

$$P_o = P_S/\sin\theta \tag{2}$$

$$\delta_p = \left(\frac{dP_o(x_d)}{dx_d}\right)_{x_d \to 0} \tag{3}$$

To contribute to P_S, a polar functional group must be oriented with its dipole perpendicular to the molecular long axis of the dopant, and it must be sterically coupled to an adjacent asymmetric center (stereopolar coupling). By reducing the conformational symmetry of the polar functional group, stereopolar coupling results in a net orientational bias of the dipole along the polar axis, thus giving rise to a spontaneous polarization. The dependence of P_S on the conformational asymmetry of chiral side chains, which comprise the vast majority of stereopolar units in chiral dopants, has been investigated in a number of different systems and is reasonably well understood.[6] Stegemeyer has shown that the polarization power of dopants with chiral side chains (e.g., **1**) is generally independent of the nature of the S_C host; these chiral dopants are classified as Type I.[8b]

Recent studies have shown that the polarization power of several new dopants with rigid chiral cores (e.g., **2**) varies with the nature of the S_C host; these dopants are classified as type II.[8] The dependence of δ_p on the nature of the S_C host has been explained on the basis of two models.[8b] In the first model, intermolecular chirality transfer leads to a polar ordering of the S_C host, which results in higher δ_p values in S_C hosts with large transverse dipole moments. In the second model, which is derived from the microscopic model of Zeks,[9] variations in δ_p arise from different rotational distributions of the dopant

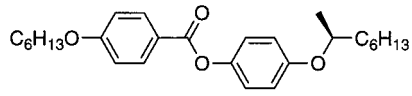

1

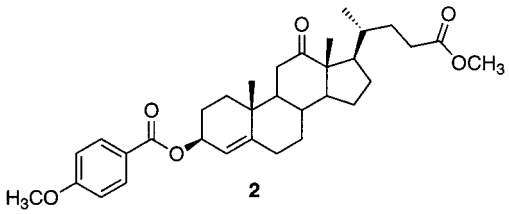

2

transverse dipole with respect to the polar axis due to so-called *hard core* (steric) interactions with the S_C host. However, due to the limited amount of experimental data reported for type II dopants, it is difficult to fully assess the validity of each model. To further investigate the host dependence of type II chiral dopants, and possibly exploit this phenomenon in the formulation of fast-switching FLC mixtures through the design of dopants with increasingly high polarization power,[10] we have undertaken the study of a new class of axially chiral dopants with atropisomeric biphenyl cores.

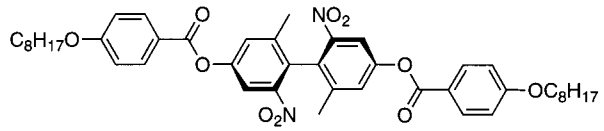

3

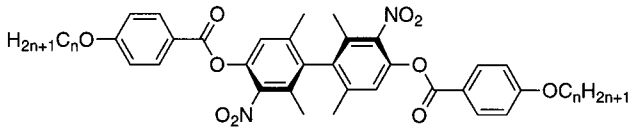

4

a, n = 1; **b**, n = 4; **c**, n = 6; **d**, n = 8; **e**, n = 9; **f**, n = 12; **g**, n = 14; **h**, n = 16; **i**, n = 18; **j**, n = 20

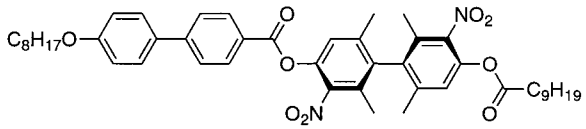

5

Only a few examples of axially chiral S_C* mesogens are known; these include allene[11] and alkylidenecyclohexane derivatives,[12] butadiene iron tricarbonyl complexes,[13] and atropi-

(5) Siemensmeyer, K.; Stegemeyer, H. *Chem. Phys. Lett.* **1988**, *148*, 409.

(6) Walba, D. M. In *Advances in the Synthesis and Reactivity of Solids*; Mallouck, T. E., Ed.; JAI Press: Ltd.: Greenwich, CT, 1991; Vol. 1.

(7) (a) Goodby, J. W.; Chin, E.; Leslie, T. M.; Geary, J. M.; Patel, J. S. *J. Am. Chem. Soc.* **1986**, *108*, 4729. (b) Goodby, J. W.; Chin, E. *J. Am. Chem. Soc.* **1986**, *108*, 4736.

(8) (a) Osipov, M. A.; Stegemeyer, H.; Sprick, A. *Phys. Rev. E* **1996**, *54*, 6387. (b) Stegemeyer, H.; Meister, R.; Hoffmann, U.; Sprick, A.; Becker, A. *J. Mater. Chem.* **1995**, *5*, 2183 and references therein. (c) Vizitiu, D.; Halden, B. J.; Lemieux, R. P. *Chem. Commun.* **1997**, 1123. (d) Yang, K.; Campbell, B.; Birch, G.; Williams, V. E.; Lemieux, R. P. *J. Am. Chem. Soc.* **1996**, *118*, 9557.

(9) Urbanc, B.; Zeks, B. *Liq. Cryst.* **1989**, *5*, 1075.

(10) For examples of chiral dopants with high polarization power, see: (a) Ikemoto, T.; Sakashita, K.; Kageyama, Y.; Terada, F.; Nakaoka, Y.; Ichimura, K.; Mori, K. *Chem. Lett.* **1992**, 567. (b) Dübal, H. R.; Escher, C.; Günther, D.; Hemmerling, W.; Inogushi, Y.; Müller, I.; Murakami, M.; Ohlendorf, D.; Wingen, R. *Jpn. J. Appl. Phys.* **1988**, *27*, L2241. (c) Nishide, K.; Nakayama, A.; Kusumoto, T.; Hiyama, T.; Takehara, S.; Shoji, T.; Osawa, M.; Kuriyama, T.; Nakamura, K.; Fujisawa, T. *Chem. Lett.* **1990**, 623. (d) Kusumoto, T.; Sato, K.; Ogino, K.; Hiyama, T.; Takehara, S.; Osawa, M.; Nakamura, K. *Liq. Cryst.* **1993**, *14*, 727. (e) Sakashita, K.; Ikemoto, T.; Nakaoka, Y.; Terada, F.; Sako, Y.; Kageyama, Y.; Mori, K. *Liq. Cryst.* **1993**, *13*, 71. (f) Kobayashi, S.; Ishibashi, S.; Takahashi, K.; Tsuru, S.; Yamamoto, F. *Adv. Mater.* **1993**, *5*, 167. (g) Ikemoto, T.; Kageyama, Y.; Onuma, F.; Shibuya, Y.; Ichimura, K.; Sakashita, K.; Mori, K. *Liq. Cryst.* **1994**, *17*, 729.

(11) (a) Lunkwitz, R.; Tschierske, C.; Langhoff, A.; Geisselmann, F.; Zugenmaier, P. *J. Mater. Chem.* **1997**, *7*, 1713. (b) Stichler-Bonaparte, J.; Kruth, H.; Lunkwitz, R.; Tschierske, C. *Liebigs Ann.* **1996**, 1375.

(12) Poths, H.; Schonfeld, A.; Zentel, R.; Kremer, F.; Siemensmeyer, K. *Adv. Mater.* **1992**, *4*, 351.

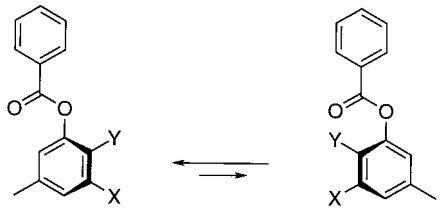

Figure 2. Structures representing two conformational minima of 3-methyl-5-nitrophenyl benzoate (X = NO_2, Y = H) and 3,5-dimethyl-2-nitrophenyl benzoate (X = Me, Y = NO_2) according to AM1 calculations.

someric 5,7-dihydro-1,11-dimethyldibenzo[*c*,*e*]thiepine derivatives.[14] In the first three cases, relatively small P_S values ranging from 12 to 38 nC/cm^2 were reported for the neat S_C* liquid crystals; no P_S data were reported for the fourth one. Our first report of ferroelectric induction by an atropisomeric dopant focused on compound **3**, which exhibited a pronounced type II behavior in the S_C hosts **PhB** and **NCB76**.[8d] We proposed that polar ordering of dopant **3** in the S_C lattice originates from a very small conformational energy bias associated with rotation of the biphenyl core about the ester C−O bond (Figure 2), which was estimated by AM1 calculations on the model compound 3-methyl-5-nitrophenyl benzoate to be 0.4 kcal/mol. We have extended this conformational analysis to other phenyl benzoate model compounds and found that shifting the symmetry-breaking NO_2 group to the 2-position raises the conformational energy bias to 1.2 kcal/mol, as shown in Figure 3. According to our hypothesis, this should result in a higher polarization power for the corresponding atropisomeric dopant. To test the validity of this conformational analysis in predicting relative δ_p values in chiral dopants with atropisomeric cores, and to investigate the origin(s) of the observed type II host dependence, we have synthesized the atropisomeric dopants **4a**−**j** and **5** and measured their polarization power in five S_C liquid crystal hosts representing four distinct structural classes of mesogens.

Results and Discussion

The atropisomeric dopants **4a**−**j** were obtained by diesterification of the optically pure dihydroxybiphenyl **8** using the corresponding 4-alkoxybenzoic acids. The dihydroxybiphenyl **8** was first obtained as a racemic mixture by conversion of the known tetramethylbenzidene **6**[15] to the dihydroxybiphenyl **7** via the bis-diazonium salt, followed by dinitration under mild conditions (Scheme 1). Resolution of **8** was achieved by semipreparative chiral stationary-phase HPLC using a Daicel Chiralcel OJ column to give both enantiomers in optically pure form. The unsymmetrical dopant **5** was obtained by monoesterification of racemic **8** using 4′-octyloxy-4-biphenylcarboxylic acid to give **9**, which was resolved by semipreparative chiral stationary-phase HPLC and esterified using decanoic acid to give **5** in optically pure form.

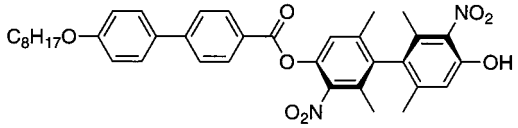

9

The dopants **4a**−**j** were mixed into the S_C hosts **PhB**, **NCB76**, **DFT**, and **PhP1** (Figure 4) over the mole fraction range 0.005 $< x_d \leq 0.05$ to give an induced S_C* liquid crystal phase.[16] Each mixture was introduced into a polyimide-coated ITO glass cell with a 4 μm gap and aligned by slow cooling from the isotropic liquid phase to the S_C* phase at 5 K below the S_C*−S_A* phase transition temperature ($T - T_C = -5$ K). Spontaneous polarization and tilt angle values were measured as a function of x_d by the triangular wave method (80−100 Hz, 6V/μm), and P_o values were calculated using eq 2. At least four different samples were prepared for each dopant−host combination.

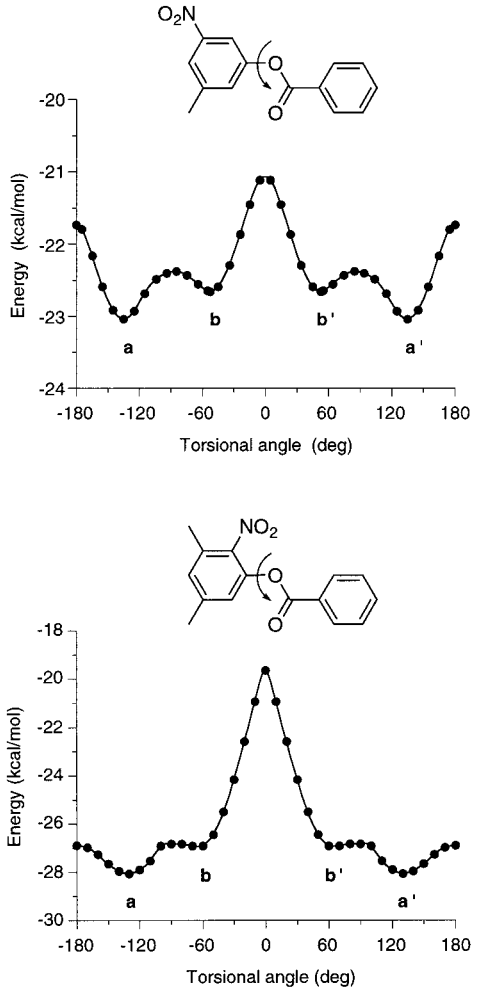

Figure 3. Energy profiles for 3-methyl-5-nitrophenyl benzoate (top) and 3,5-dimethyl-2-nitrophenyl benzoate (bottom) as a function of the torsional angle defined by C-6, C-1, O, C(O) and C-2, C-1, O, C(O), respectively, according to AM1 calculations.

Scheme 1[a]

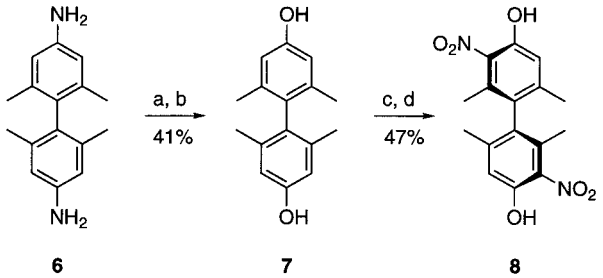

[a] Key: (a) $NaNO_2$, 10% H_2SO_4, 5 °C; (b) reflux; (c) $Fe(NO_3)_3 \cdot 9H_2O$, EtOH; (d) chiral stationary-phase HPLC resolution, Daicel Chiralcel OJ column, 9:1 hexanes/EtOH, 3 mL/min.

(13) Jacq, P.; Malthete, J. *Liq. Cryst.* **1996**, *21*, 291.
(14) Solladié, G.; Hugelé, P.; Bartsch, R. *J. Org. Chem.* **1998**, *63*, 3895.
(15) Carlin, R. B. *J. Am. Chem. Soc.* **1945**, *67*, 928.

(16) Doping compounds **3**−**5** into any of the S_C hosts caused the temperature range of the resulting S_C* phase to decrease with increasing dopant mole fraction, thus limiting the useful range to $x_d \leq 0.05$.

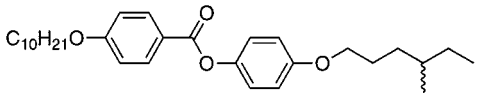

PhB; phase sequence: Cr 35 S_C 70.5 S_A 72 N 75 I

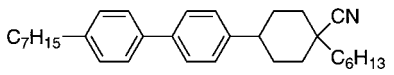

NCB76; phase sequence: Cr 66 (S_G 55) S_C 73 S_A 117 N 125 I

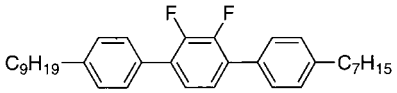

DFT; phase sequence: Cr 49 S_C 77 S_A 93 N 108 I

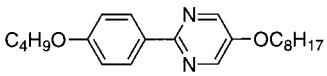

PhP1; phase sequence: Cr 58 S_C 85 S_A 95 N 98 I

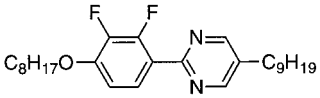

PhP2; phase sequence: Cr 42 S_C 52 I

Figure 4. Structures of liquid crystal hosts and phase transition temperatures in °C.

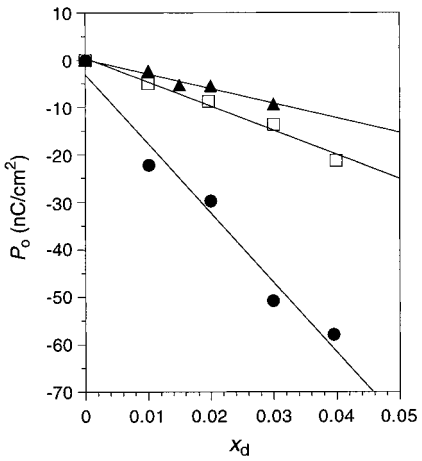

Figure 5. Reduced polarization P_o as a function of dopant mole fraction x_d for the dopant (−)-**4e** in the S_C hosts **DFT** (triangles), **NCB76** (squares), and **PhP1** (circles) at $T - T_C = -5$ K.

Plots of P_o vs x_d gave good linear fits, as shown in Figure 5 for dopant (−)-**4e**, from which δ_p values were obtained according to eq 3. These results are presented in Table 1, along with new data for dopant (−)-**3** in **DFT** and **PhP1**. As previously observed with dopant (−)-**3**,[8d] dopants in series **4** with short to medium chain lengths, except for (−)-**4c**, produced no measurable spontaneous polarization in the S_C host **PhB** even though the characteristic Goldstone-mode switching of a S_C* phase was evident upon applying an AC field across the cell. Upper limit values for δ_p were estimated from tilt angle measurements at $T - T_C = -5$ K assuming a detection limit of 0.3 nC/cm^2 at a maximum dopant mole fraction of 0.05. Measurable spontaneous polarizations were obtained in **PhB** for dopants with chain lengths C_{12} and longer. All dopants gave a measurable spontaneous polarization in the other three S_C hosts, except for (−)-**4a** in **DFT** and **PhP1** and (+)-**4b** in **DFT**. The results in Table 1 show that the sign of P_S induced by **4a**−**j** in the S_C hosts **DFT**, **NCB76**, and **PhP1** correlates with the relative configuration of the atropisomeric core: all dopants derived from (+)-**8** induced a positive polarization and all those derived from (−)-**8** induced a negative polarization. In **PhB**, P_S sign inversions were observed for the C_4−C_8 derivatives (+)-**4b**,**d** and (−)-**4c**.

Table 1. Polarization Power δ_p of Dopants **3** and **4a**−**j** in the S_C Hosts **PhB**, **DFT**, **NCB76**, and **PhP1** Measured at $T - T_C = -5$ K

	δ_p[a,b] (nC/cm^2)			
dopant	**PhB**	**DFT**	**NCB76**	**PhP1**
(−)-**3**	<20 (−)[c,d]	63 (+)[e]	170 (+)[c]	161 ± 11 (+)
(−)-**4a**	<30[d,g]	<27 (−)[d]	103 ± 14 (−)	<43 (−)[d]
(+)-**4b**	<30 (−)[d]	<30 (+)[d]	183 ± 6 (+)	505 ± 51 (+)
(−)-**4c**	171 ± 11 (+)	98 (−)[e]	274 ± 12 (−)	1199 ± 81 (−)
(+)-**4d**	<30 (−)[d]	124 (+)[e]	373 ± 54 (+)	1738 ± 95 (+)
(−)-**4e**	<34 (−)[d]	312 ± 32 (−)	514 ± 38 (−)	1555 ± 119 (−)
(+)-**4f**	250 ± 11 (+)	602 ± 37 (+)	768 ± 23 (+)	1423 ± 149 (+)
(−)-**4g**	496 ± 43 (−)	817 ± 54 (−)	856 ± 73 (−)	1392 ± 140 (−)
(+)-**4h**	449 ± 42 (+)	550 ± 44 (+)	940 ± 71 (+)	1329 ± 60 (+)
(+)-**4i**	506 ± 8 (+)	500 ± 78 (+)	634 ± 70 (+)	998 ± 18 (+)
(−)-**4j**	388 (−)[e]	454 ± 39 (−)	280 ± 26 (−)	*f*

[a] Sign of induced P_S in parentheses. [b] Uncertainty is ± standard error of least-squares fit. [c] From ref 8d. [d] Estimated upper limit based on a detection limit of 0.3 nC/cm^2 at the highest dopant mole fraction. [e] Values extrapolated from a single P_o measurement at $x_d = 0.03$−0.04. [f] The temperature range of the S_C* phase was less than 5 K. [g] Unable to determine the sign of P_S.

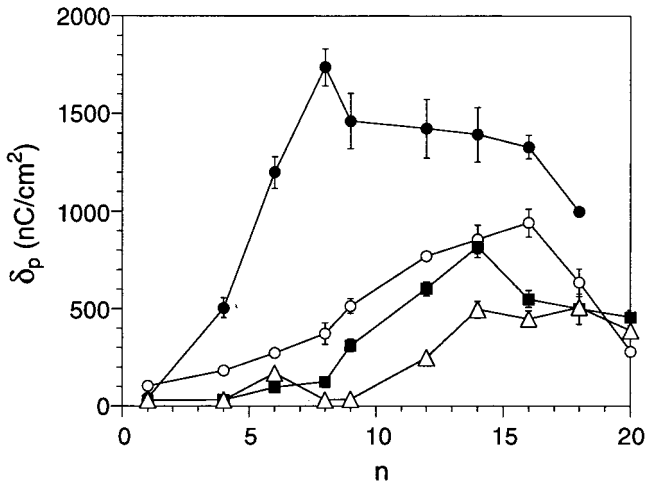

Figure 6. Polarization power δ_p as a function of alkoxy chain length n for dopants **4a**−**j** in the S_C hosts **PhB** (triangles), **DFT** (squares), **NCB76** (circles), and **PhP1** (filled circles). Error bars represent ±SE.

Inspection of the results in Table 1 reveals three important trends. First, the polarization power of the 2,2′-dinitro dopant (−)-**3** is significantly less than that of the corresponding 3,3′-dinitro dopant (+)-**4d** in **NCB76**, **DFT,** and **PhP1**, which is consistent with an increase in the conformational energy bias for rotation about the ester C−O bond (vide supra). Second, the polarization power of all dopants strongly depends on the nature of the S_C host, as predicted by Stegemeyer et al., although on a larger scale than reported heretofore.[8b] For example, the polarization power of (+)-**4d** in **PhP1** is at least 55 times that estimated for (+)-**4d** in **PhB**. Third, the polarization power of dopants in series **4** varies with the length of the alkoxy chains, as shown in Figure 6. The highest polarization power was recorded in the S_C host **PhP1** for the C_8 derivative (+)-**4d** (+1738 nC/cm^2), which is one of the highest δ_p values reported thus far in the literature for a chiral dopant.[10] A plot of P_S vs temperature for a 2 mol % mixture of (+)-**4d** in **PhP1** (Figure

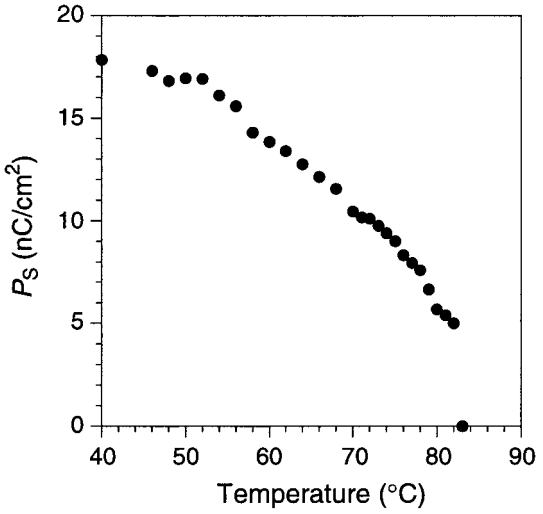

Figure 7. Spontaneous polarization P_S as a function of temperature for a 2 mol % mixture of (+)-**4d** in **PhP1**.

7) shows a supercooling of the induced S_C* phase to 40 °C (pure **PhP1** crystallizes at 58 °C) and gives a maximum spontaneous polarization P_S(max) of +18 nC/cm^2, which corresponds to an extrapolated P_S(max) value for dopant (+)-**4d** of +900 nC/cm^2.

To explain these results, we consider the models proposed for the molecular origins of Type II behavior.[8b] In a general sense, the polarization power of Type II dopants is thought to be strongly influenced by interactions between the chiral core of the dopant and the achiral cores of the surrounding host molecules. This is reasonable since the core region of a smectic liquid crystal phase is more highly ordered than the tail regions, and intermolecular interactions in the former are expected to affect macroscopic bulk properties to a much greater extent than intermolecular interactions in the latter. Such *intercore* interactions may or may not result in substantial chirality transfer depending on the complementarity of the core structures. An extension of Zeks' microscopic model[9] suggests that the spontaneous polarization induced by a type II chiral dopant is influenced by steric interactions with the surrounding S_C host molecules that affect the orientation of the core transverse dipole with respect to the polar axis (rotational distribution). The spontaneous polarization is expressed as a function of the core transverse dipole moment $\mu_\perp$ by eq 4:

$$P_S = N_1 \mu_\perp \cos \psi_o \langle \cos \psi \rangle \qquad (4)$$

where N_1 is the dopant number density, ψ_o is the angle between $\mu_\perp$ and a reference axis **m** defined by the shape of the chiral core, and $\langle \cos \psi \rangle$ is a polar order parameter ranging from 0 to 1 that is related to the conformational asymmetry of the chiral core about the molecular long axis (Figure 8).[8b] According to this model, the relatively small δ_p values obtained in **PhB** could be due to a rotational distribution that brings the transverse dipole of the chiral core near the tilt plane. In such a situation, small changes in $\langle \cos \psi \rangle$ could change the sign of P_S by rotating the vector $\mu_\perp$ through the tilt plane. This would be consistent with the fact that dopant (−)-**3** and some of the shorter chain dopants in series **4** show a sign inversion in P_S going from **PhB** to the other three S_C hosts (see Table 1). Conversely, the higher δ_p values obtained in **DFT**, **NCB76**, and **PhP1** and the lack of P_S sign inversion in these S_C hosts could be explained by a shift in rotational distribution that brings the core transverse dipole closer to the C_2 polar axis.

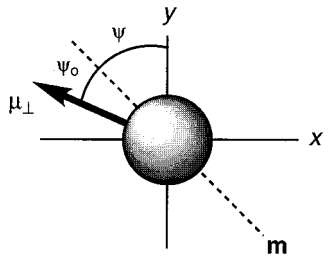

Figure 8. Schematic view of the chiral core along the molecular long axis: ψ_o is the angle between the transverse dipole $\mu_\perp$ and the molecular reference axis **m**, and ψ is the angle between **m** and the polar axis *y*. The tilt plane is in the *xz* plane.

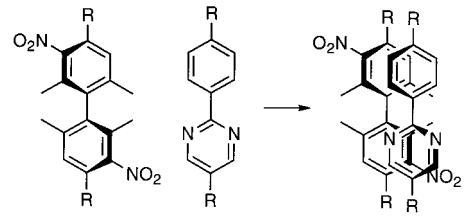

Figure 9. Model for intercore chirality transfer between the atropisomeric dopant and the S_C host **PhP1**.

However, simple calculations[17] show that the rotational distribution model alone cannot account for the wide variations in δ_p values reported in Table 1, especially the high δ_p values obtained in **PhP1**. For example, assuming $\mu_\perp$ to be coincident with the molecular reference axis ($\cos \psi_o = 1$), this model predicts a polar order parameter $\langle \cos \psi \rangle$ of 0.58 for dopant (+)-**4d** in **PhP1** at $T - T_C = -40$ K, which is remarkably large considering the relatively small degree of conformational asymmetry expected for such a dopant in the S_C lattice (vide supra).[18] In this case, it is likely that dopant−host interactions do more than simply influence the rotational distribution of the core transverse dipole; such interactions may also amplify the conformational asymmetry of the chiral dopants via chirality transfer.

Semiempirical calculations suggest that the core structures of all four S_C hosts adopt twisted chiral conformations that should be in rapid equilibrium with their enantiomeric mirror images at ambient temperature.[19] Interactions with a dopant chiral core favoring one handedness can shift such conformational equilibrium toward one of the two enantiomeric states and result, in some cases, in a nonlinear amplification of chiral bulk properties.[20] As shown in Figure 9, conformational interactions between the atropisomeric core of an orientationally ordered dopant such as **4** and the cores of neighboring S_C host molecules should result in an effective transfer of molecular chirality to favor, or induce, one twisted conformation of the S_C host.[21] In principle, this *intercore* chirality transfer could amplify the induced spontaneous polarization by (i) inducing a polar ordering of the S_C host transverse dipole,[8b] and/or (ii)

(17) Dunmur, D. A.; Grayson, M.; Roy, S. K. *Liq. Cryst.* **1994**, *16*, 95.

(18) The polar order parameter $\langle \cos \psi \rangle$ was calculated using eq 4. A $\mu_\perp$ value of 2.49D was obtained by ab initio calculation at the HF/3-21G* level on the AM1-minimized model system 4,4′-dibenzoyl-2,2′,6,6′-tetramethyl-3,3′-dinitrobiphenyl in its lowest energy conformation. The dopant number density N_1 of a 2 mol % mixture of (+)-**4d** in **PhP1** was estimated as 2% of the molecular number density of **PhP1**. The density of **PhP1** was assumed to be 1.1 g/cm^3.

(19) Low-level ab initio calculations at the STO-3G level suggest that the global minimum of 2-phenylpyrimidine, which forms the core structure of **PhP1**, adopts a planar conformation in the gas phase: Barone, V.; Commisso, L.; Lelj, F.; Russo, N. *Tetrahedron* **1985**, *41*, 1915.

(20) Green, M. M.; Zanella, S.; Gu, H.; Sato, T.; Gottarelli, G.; Jha, S. K.; Spada, G. P.; Schoevaars, A. M.; Feringa, B.; Teramoto, A. *J. Am. Chem. Soc.* **1998**, *120*, 9810.

Table 2. Polarization Power δ_p of Dopant (−)-**4e** at $T - T_C = -5$ K and Helical Pitch of the Induced S_C* Phase in the Liquid Crystal Hosts **PhB**, **DFT**, **NCB76**, and **PhP1** and a 1:1 **PhP1/PhP2** Mixture

S_C Host	δ_p[a] (nC/cm^2)	pitch[b,c] (μm)	$\mu_\perp$[d] (D)
PhB	<34[e]	4.3 ± 0.2	2.4
DFT	312 ± 32	7.4 ± 0.6	3.2
NCB76	514 ± 38	5.9 ± 0.6	3.8
PhP1	1555 ± 119	2.9 ± 0.3	0.92
1:1 **PhP1/PhP2**	1063 ± 76	1.5 ± 0.1	2.9

[a] Uncertainty is ± standard error of least-squares fit. [b] Measured at a dopant mole fraction $x_d = 0.02$. [c] Uncertainty is ± one standard deviation. [d] Transverse dipole moment of the S_C host calculated at the HF/3-21G* level. [e] Estimated upper limit based on a detection limit of 0.3 nC/cm^2 at the highest dopant mole fraction.

inducing an asymmetric distortion of the S_C lattice that would increase the conformational asymmetry of the atropisomeric core by a feedback mechanism.

An induced polar ordering of the S_C host can be ruled out as the main cause of polarization amplification by comparing δ_p values with transverse dipole moments ($\mu_\perp$) of the corresponding S_C host core structures. The latter values were obtained by single point ab initio calculations at the HF/3-21G* level using structures minimized at the semiempirical AM1 level and are listed in Table 2.[22] The results show that there is no correlation between the polarization power and the host transverse dipole moment: the highest δ_p values are obtained in the S_C host with the smallest transverse dipole moment, **PhP1**, which is inconsistent with polar ordering of the S_C host. The polarization power of (−)-**4e** was also measured in a 1:1 mixture of **PhP1** and the difluoro derivative **PhP2**, which has a transverse dipole moment of 5.03 D in its lowest energy conformation. In the 1:1 mixture, the dopant (−)-**4e** gave a polarization power of −1063 nC/cm^2, which is about 30% less than that obtained in pure **PhP1**.[23] This is also inconsistent with polar ordering of the S_C host and suggests that polarization amplification in **PhP1** may be due in large part to an increase in conformational asymmetry of the dopant as a result of intercore chirality transfer.

To assess the importance of intercore chirality transfer in polarization amplification, the polarization power of the unsymmetrical dopant (−)-**5** was measured in the S_C host **PhP1**. Although (−)-**5** has the same length as the symmetrical dopant (+)-**4d**, the position of its atropisomeric core should be offset with respect to the core region of the S_C layer on the time average. As a result of this positional shift, and the expected reduction in chiral conformational interactions between the core of the dopant and those of the surrounding host molecules, the polarization power of (−)-**5** should be lower than that of the symmetrical dopant (+)-**4d**. Indeed, the polarization power of (−)-**5** proved to be ca. 35% less than that obtained for (+)-**4d**: −1101 nC/cm^2 vs +1738 nC/cm^2, respectively. Furthermore, a comparison of S_C* helical pitch values for 2 mol % mixtures in **PhP1** showed that (+)-**4d** induces a tighter helical pitch than (−)-**5**, which is also consistent with a decrease in dopant-host chirality transfer: 1.5 ± 0.3 μm vs 2.4 ± 0.5 μm, respectively.

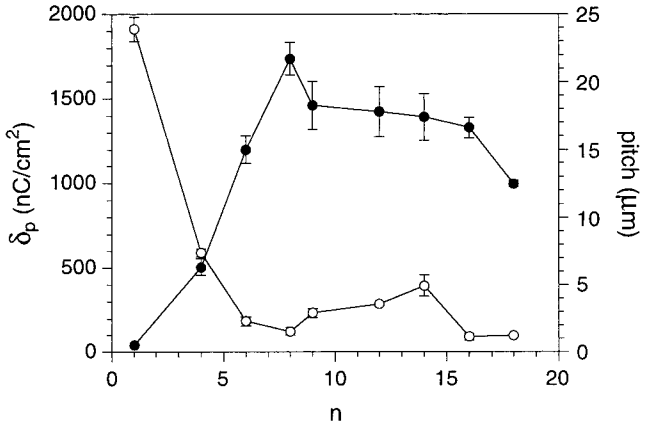

Figure 10. Polarization power δ_p (filled circles) and S_C* helical pitch (circles) as a function of alkoxy chain length *n* for dopants **4a**−**i** in the S_C host **PhP1**. Error bars represent ±SE (δ_p) and ±one standard deviation (pitch).

Another way to assess the importance of intercore chirality transfer is to study the effect of varying the length of the dopant side chains on the polarization power. As shown in Figure 6, the polarization power of dopant **4** increases with increasing alkoxy chain length *n* in all four S_C hosts, reaching a maximum at a value *n*(max) that varies with the S_C host. The subsequent decrease in δ_p with a further increase in *n* has been observed before with some type I dopants but remains largely unexplained.[24] The increase in δ_p with increasing chain length is consistent with an increase in positional/orientational ordering of the atropisomeric core in the S_C lattice, which should improve intercore chirality transfer as well as increase the contribution of the ester asymmetric conformational mode toward polar ordering by *anchoring* the side chains in the transoid S_C lattice.[25] The variation in *n*(max) as a function of the S_C host may be related to differences in the S_C layer spacing and/or differences in the length of the S_C host core structure. Measurements of S_C* helical pitch were also carried out for 2 mol % mixtures of **4a**−**i** in **PhP1**. As shown in Figure 10, the S_C* helical pitch follows a trend that is opposite to that followed by δ_p as a function of *n*, except at very long chain lengths. This observation further supports the claim that polarization amplification in **PhP1** is strongly linked to intercore chirality transfer.

However, when the S_C* helical pitch is measured as a function of the S_C host (Table 2), we find that there is essentially no correlation between the S_C* pitch and δ_p. Given these and other experimental results presented herein, we conclude that one cannot rationalize the variations in polarization power as a function of the S_C host on the basis of a single microscopic model. Indeed, the two models described above are not mutually exclusive, and it is likely that differences in δ_p values for an atropisomeric dopant in any two S_C hosts can be explained by variations in both the rotational distribution of the transverse dipole and intercore chirality transfer. Nevertheless, the results obtained in **PhP1** may be singled out as a unique case in which intercore chirality transfer plays a key role in amplifying the induced spontaneous polarization. We propose that polarization amplification takes place via a feedback mechanism in which intercore chirality transfer results in an asymmetric distortion

(21) A similar mechanism of chiral induction was proposed for cholesteric phases induced by atropisomeric biaryl dopants in order to account for the correlation found between helical twist sense of the cholesteric phase and that of the dopant: Gottarelli, G.; Hibert, M.; Samori, B.; Solladié, G.; Spada, G. P.; Zimmermann, R. *J. Am. Chem. Soc.* **1983**, *105*, 7318.

(22) A plot of experimental dipole moments vs dipole moments calculated at the HF/3-21G* level for a series of monosubstituted benzenes gave an excellent linear correlation ($R^2 = 0.994$).

(23) The decrease in δ_p may be ascribed to a difference in polarizability anisotropy of the phenylpyrimidine cores that should, in principle, affect the strength of dopant/host chiral conformational interactions. A systematic investigation of this relationship is underway, and results will be published elsewhere.

(24) Loseva, M.; Chernova, N.; Rabinovitch, A.; Poshidaev, E.; Narkevitch, J.; Petrashevitch, O.; Kazachkov, E.; Korotkova, N.; Schadt, M.; Bucheker, R. *Ferroelectrics* **1991**, *114*, 357.

(25) A similar effect was reported for a more conventional type I dopant and accounted for by considering the "rotational damping" of the stereopolar unit with increasing chain length: Goodby, J. W.; Patel, J. S.; Chin, E. *J. Phys. Chem.* **1987**, *91*, 5151.

of the S_C* lattice that, in turn, further increases the conformational asymmetry of the atropisomeric dopant by virtue of increased diastereomeric bias between the S_C* lattice and the chiral conformations of the dopant. Further studies aimed at providing additional experimental and theoretical support for this hypothesis are in progress.

Experimental Section

General Methods. ^{1}H and ^{13}C NMR spectra were recorded on Bruker ACF-200 and AM-400 NMR spectrometers in deuterated chloroform ($CDCl_3$) and deuterated dimethyl sulfoxide (DMSO-d_6). The chemical shifts are reported in δ (ppm) relative to tetramethylsilane as internal standard. Low-resolution EI mass spectra were recorded on a Fisons VG Quattro triple quadrupole mass spectrometer; peaks are reported as *m*/*z* (percent intensity relative to the base peak). High-resolution EI mass spectra were performed by the University of Ottawa Regional Mass Spectrometry Center. Optical rotations were measured on a Perkin-Elmer 241 polarimeter at room temperature. Semipreparative chiral stationary-phase HPLC separations were performed using a 25 cm × 10 mm i.d. Daicel Chiralcel OJ column. Elemental analyses were performed by Guelph Chemical Laboratories Ltd (Guelph, Ontario) and by MHW Laboratories (Phoenix, AZ). Melting points were measured on a Mel-Temp II melting point apparatus and are uncorrected.

Materials. All reagents, chemicals, and liquid crystal hosts were obtained from commercial sources and used without further purification unless otherwise noted. Methylene chloride (CH_2Cl_2) was distilled from P_2O_5 under N_2. Tetrahydrofuran (THF) was distilled from sodium/benzophenone under N_2. (−)-2,2′-Dimethyl-6,6′-dinitro-4,4′-bis[(4-octyloxybenzoyl)oxy]biphenyl ((−)-**3**),[8d] 4,4′-diamino-2,2′,6,6′-tetramethylbiphenyl (**6**),[15] (±)-4-[(4-methylhexyl)oxy]phenyl 4-decyloxybenzoate (**PhB**),[26] 2′,3′-difluoro-4-heptyl-4″-nonyl-*p*-terphenyl (**DFT**),[27] and 4-octyloxy-4′-biphenylcarboxylic acid[28] were synthesized according to published procedures and shown to have the expected physical and spectral properties. The liquid crystal host **NCB76** was provided by Prof. H. Stegemeyer.

4,4′-Dihydroxy-2,2′,6,6′-tetramethylbiphenyl (7). A solution of $NaNO_2$ (0.27 g, 4.0 mmol) in H_2O (2 mL) was added dropwise to a solution of **6** (0.48 g, 2.0 mmol) in 10% aqueous H_2SO_4 (10 mL) cooled to 5 °C. The mixture was stirred at 5 °C for 30 min, then refluxed with stirring overnight. After cooling, the mixture was extracted with EtOAc (2 × 20 mL), and the combined extracts were washed with H_2O and brine, dried ($MgSO_4$), and concentrated. The solid residue was purified by sublimation (0.06 Torr, 125 °C) to give 0.20 g (41%) of **7** as a white solid: mp 172−174 °C (lit.[29] mp 183 °C); ^{1}H NMR (200 MHz, DMSO-d_6) δ 1.73 (s, 12H), 6.52 (s, 4H), 9.05 (s, 2H); ^{13}C NMR (50 MHz, DMSO-d_6) δ 19.7, 114.2, 130.1, 136.4, 155.5; MS (EI) *m*/*z* 242 (M^+, 100), 227 (64), 212 (74) 105 (28); HRMS (EI) calcd for $C_{16}H_{18}O_2$ 242.1307, found 242.1302.

(−)- and (+)-4,4′-Dihydroxy-2,2′,6,6′-tetramethyl-3,3′-dinitrobiphenyl ((−)-8 and (+)-8). A mixture of **6** (2.16 g, 8.95 mmol) and $Fe(NO_3)_3$·$9H_2O$ (2.53 g, 6.26 mmol) in absolute EtOH (60 mL) was refluxed with stirring overnight. After cooling, the mixture was concentrated to a solid residue that was dissolved in EtOAc (20 mL), washed with 2 M aqueous HCl, water, and brine, dried ($MgSO_4$), and concentrated. Purification by flash chromatography on silica gel ($CHCl_3$) gave 1.39 g (47%) of (±)-**8** as a bright yellow solid. After recrystallization from 10% $CHCl_3$/hexanes, the product was resolved by semipreparative chiral stationary-phase HPLC (9:1 hexanes/EtOH, 3 mL/min). The first eluant was collected and concentrated to give (−)-**8** in optically pure form: mp 128−130 °C; $[\alpha]_D$ −99.4 (*c* 1.1, $CHCl_3$); ^{1}H NMR (400 MHz, $CDCl_3$) δ 1.89 (s, 6H) 2.16 (s, 6H), 7.01 (s, 2H), 10.04 (s, 2H); ^{13}C NMR (100 MHz, $CDCl_3$) δ 18.0, 21.0, 118.6, 132.1, 134.2, 134.8, 145.7, 153.9; MS (EI) *m*/*z* 332 (M+, 100), 315 (87), 165 (67), 152 (65), 128 (75), 115 (88); HRMS (EI) calcd for $C_{16}H_{16}N_2O_6$ 332.1008, found 332.1015. The second eluant was collected and concentrated to give (+)-**8** in optical purity of 96% ee.

General Procedure for the Preparation of Dopants 4a−i. The procedure described for the preparation of (−)-2,2′,6,6′-tetramethyl-3,3′-dinitro-4,4′-bis[(4-nonyloxybenzoyl)oxy]biphenyl ((−)-**4e**) is representative. Dopants (−)-**4a**,**c**,**e**,**g** were derived from (−)-**8**; dopants (+)-**4b**,**d**,**f**,**h**,**i** were derived from (+)-**8**.

Under an Ar atmosphere, solid DCC (35 mg, 0.17 mmol) was added to a stirred solution of (−)-**8** (26 mg, 0.08 mmol), 4-nonyloxybenzoic acid (45 mg, 0.17 mmol) and DMAP (21 mg, 0.17 mmol) in dry CH_2Cl_2 (5 mL). The mixture was stirred at room temperature for 24 h and then filtered and concentrated. The solid residue was redissolved in EtOAc, washed with 2 M aqueous HCl, H_2O, and brine, dried ($MgSO_4$), and concentrated. Purification by flash chromatography on silica gel (7:3 hexanes/EtOAc) gave 56 mg (88%) of (−)-**4e** as a white solid. Prior to doping into liquid crystal hosts, the compound was recrystallized from hexanes after filtration through a 0.45 μm PTFE filter: mp 116−118 °C; $[\alpha]_D$ −7.32 (*c* 1.1, $CHCl_3$); ^{1}H NMR (400 MHz, $CDCl_3$) δ 0.89 (t, J = 7.0 Hz, 6H), 1.30−1.54 (m, 24H), 1.76−1.89 (m, 4H), 1.99 (s, 6H), 2.03 (s, 6H), 4.05 (t, J = 6.5 Hz, 4H), 6.97 (d, J = 8.9 Hz, 4H), 7.34 (s, 2H), 8.08 (d, J = 8.9 Hz, 4H); ^{13}C NMR (100 MHz, $CDCl_3$) δ 14.1, 15.1, 20.4, 22.7, 26.0, 29.1, 29.3, 29.4, 29.5, 31.9, 68.4, 114.6, 120.0, 123.6, 129.7, 132.7, 136.2, 140.0, 142.0, 143.4, 163.6, 164.1.

Anal. Calcd for $C_{48}H_{60}N_2O_{10}$: C, 69.88; H, 7.33; N, 3.40. Found: C, 69.69; H, 7.13; N, 3.17.

(−)-4,4′-Bis[(4-methoxybenzoyl)oxy]-2,2′,6,6′-tetramethyl-3,3′-dinitrobiphenyl ((−)-4a): white solid (80%); mp 185−186 °C; ^{1}H NMR (400 MHz, $CDCl_3$) δ 1.99 (s, 6H), 2.03 (s, 6H), 3.90 (s, 6H), 7.00 (d, J = 8.8 Hz, 4H), 7.34 (s, 2H), 8.10 (d, J = 8.8 Hz, 4H); ^{13}C NMR (100 MHz, $CDCl_3$) δ 15.1, 20.4, 55.6, 114.1, 120.3, 123.5, 129.7, 132.7, 136.2, 140.0, 141.9, 143.4, 163.5, 164.4.

(+)-4,4′-Bis[(4-butyloxybenzoyl)oxy]-2,2′,6,6′-tetramethyl-3,3′-dinitrobiphenyl ((+)-4b): white needles (40%); mp 155−157 °C; ^{1}H NMR (400 MHz, $CDCl_3$) δ 1.00 (t, J = 7.4 Hz, 6H), 1.46−1.61 (m, 4H), 1.74−1.89 (m, 4H), 1.99 (s, 6H), 2.03 (s, 6H), 4.06 (t, J = 6.5 Hz, 4H), 6.98 (d, J = 8.8 Hz, 4H), 7.34 (s, 2H), 8.08 (d, J = 8.8 Hz, 4H); ^{13}C NMR (100 MHz, $CDCl_3$) δ 13.8, 15.1, 19.2, 20.4, 31.1, 68.1, 114.5, 119.9, 123.5, 129.7, 132.7, 136.1, 140.0, 141.9, 143.4, 163.6, 164.1.

(−)-4,4′-Bis[(4-hexyloxybenzoyl)oxy]-2,2′,6,6′-tetramethyl-3,3′-dinitrobiphenyl ((−)-4c): white needles (71%); mp 120−122 °C; ^{1}H NMR (400 MHz, $CDCl_3$) δ 0.92 (t, J = 6.8 Hz, 6H), 1.34−1.50 (m, 12H), 1.75−1.89 (m, 4H), 4.05 (t, J = 6.5 Hz, 4H), 6.98 (d, J = 8.8 Hz, 4H),7.34 (s, 2H), 8.08 (d, J = 8.8 Hz, 4H); ^{13}C NMR (100 MHz, $CDCl_3$) δ 14.0, 15.1, 20.4, 22.6, 25.6, 29.0, 31.5, 68.4, 114.5, 119.9, 123.5, 129.7, 132.6, 136.1, 140.0, 141.9, 143.3, 163.6, 164.1.

(+)-2,2′,6,6′-Tetramethyl-3,3′-dinitro-4,4′-bis[(4-octyloxybenzoyl)-oxy]biphenyl ((+)-4d): white needles (44%); mp 112−114 °C; ^{1}H NMR (400 MHz, $CDCl_3$) δ 0.90 (t, J = 6.7 Hz, 6H), 1.30−1.55 (m, 20H), 1.76−1.89 (m, 4H), 1.99 (s, 6H), 2.03 (s, 6H),4.05 (t, J = 6.5 Hz, 4H), 6.97 (d, J = 8.8 Hz, 4H), 7.34 (s, 2H), 8.08 (d, J = 8.8 Hz, 4H); ^{13}C NMR (100 MHz, $CDCl_3$) δ 14.1, 15.1, 20.4, 22.6, 26.0, 29.0, 29.2, 29.3, 31.8, 68.4, 114.5, 120.0, 123.5, 129.7, 132.7, 136.1, 140.0, 142.0, 143.4, 163.6, 164.1.

(+)-4,4′-Bis[(4-dodecyloxybenzoyl)oxy]-2,2′,6,6′-tetramethyl-3,3′-dinitrobiphenyl ((+)-4f): white solid (71%); mp 92−94 °C; ^{1}H NMR (400 MHz, $CDCl_3$) δ 0.89 (t, J = 6.7 Hz, 6H), 1.27−1.50 (m, 36H), 1.75−1.89 (m, 4H), 1.99 (s, 6H), 2.03 (s, 6H), 4.05 (t, J = 6.5 Hz, 4H), 6.97 (d, J = 8.8 Hz, 4H), 7.34 (s, 2H), 8.08 (d, J = 8.8 Hz, 4H); ^{13}C NMR (100 MHz, $CDCl_3$) δ 14.1, 15.1, 20.4, 22.7, 26.0, 29.0, 29.4, 29.55, 29.58, 29.64, 31.9, 68.4, 114.5, 119.9, 123.6, 129.7, 132.7, 136.1, 140.0, 141.9, 143.4, 163.6, 164.1.

(−)-2,2′,6,6′-Tetramethyl-3,3′-dinitro-4,4′-bis[(4-tetradecyloxybenzoyl)oxy]biphenyl ((−)-4g): white solid (52%); mp 94−96 °C; ^{1}H NMR (400 MHz, $CDCl_3$) δ 0.88 (t, J = 6.7 Hz, 6H), 1.26−1.49 (m, 44H), 1.78−1.89 (m, 4H), 1.99 (s, 6H), 2.03 (s, 6H), 4.05 (t, J = 6.5 Hz, 4H), 6.99 (d, J = 8.9 Hz, 4H), 7.34 (s, 2H), 8.10 (d, J = 8.9 Hz, 4H); ^{13}C NMR (100 MHz, $CDCl_3$) δ 14.1, 15.1, 20.4, 22.7, 26.0, 29.0, 29.4, 29.55, 29.59, 29.66, 31.9, 68.4, 114.5, 119.9, 123.6, 129.7, 132.7, 136.1, 140.0, 141.9, 143.4, 163.6, 164.1.

(26) Keller, P. *Ferroelectrics* **1984**, *58*, 3.
(27) Gray, G. W.; Hird, M.; Lacey, D.; Toyne, K. J. *J. Chem. Soc., Perkin Trans. 2* **1989**, 2041.
(28) Gray, G. W.; Hartley, J. B.; Jones, B. *J. Chem. Soc.* **1955**, 1412.
(29) Nomura, Y.; Takeuchi, Y. *J. Chem. Soc. B* **1970**, 956.

(+)-4,4′-Bis[(4-hexadecyloxybenzoyl)oxy]-2,2′,6,6′-tetramethyl-3,3′-dinitrobiphenyl ((+)-4h): white solid (14%); mp 88−90 °C; ^{1}H NMR (400 MHz, $CDCl_3$) δ 0.88 (t, J = 6.7 Hz, 6H), 1.26−1.50 (m, 52H), 1.78−1.89 (m, 4H), 1.99 (s, 6H), 2.03 (s, 6H), 4.05 (t, J = 6.5 Hz, 4H), 6.97 (d, J = 8.8 Hz, 4H), 7.34 (s, 2H), 8.08 (d, J = 8.8 Hz, 4H); ^{13}C NMR (100 MHz, $CDCl_3$) δ 14.1, 15.1, 20.4, 22.7, 26.0, 29.1, 29.4, 29.57, 29.60, 29.66, 31.9, 68.4, 114.5, 119.9, 123.6, 129.7, 132.7, 136.1, 140.0, 141.9, 143.4, 163.6, 164.1.

(+)-4,4′-Bis[(4-octadecyloxybenzoyl)oxy]-2,2′,6,6′-tetramethyl-3,3′-dinitrobiphenyl ((+)-4i): white solid (65%): mp 90−92 °C; ^{1}H NMR (400 MHz, $CDCl_3$) δ 0.88 (t, J = 6.7 Hz, 6H), 1.26−1.50 (m, 60H), 1.78−1.89 (m, 4H), 1.99 (s, 6H), 2.03 (s, 6H), 4.05 (t, J = 6.5 Hz, 4H), 6.97 (d, J = 8.8 Hz, 4H), 7.34 (s, 2H), 8.08 (d, J = 8.8 Hz, 4H); ^{13}C NMR (100 MHz, $CDCl_3$) δ 14.1, 15.1, 20.4, 22.7, 26.0, 29.1, 29.4, 29.57, 29.60, 29.66, 31.9, 68.4, 114.5, 119.9, 123.6, 129.7, 132.7, 136.1, 140.0, 141.9, 143.4, 163.6, 164.1.

(−)-4,4′-Bis[(4-eicosanoyloxybenzoyl)oxy]-2,2′,6,6′-tetramethyl-3,3′-dinitrobiphenyl ((−)-4j). Under an Ar atmosphere, thionyl chloride (1.0 mL, 13 mmol) was added dropwise to a mixture of 4-eicosanoyloxybenzoic acid (20 mg, 0.048 mmol) and dry benzene (2 mL) at room temperature. After the mixture was refluxed for 2 h, it was concentrated to give the 4-eicosanoyloxybenzoyl chloride as a colorless oil. Under an Ar atmosphere, a solution of (−)-**8** (7 mg, 0.022 mmol) and DMAP (6 mg, 0.049 mmol) in dry THF (5 mL) was added to the acid chloride. The mixture was stirred at room temperature overnight, diluted with EtOAc (20 mL), washed with 2 M aqueous HCl, H_2O, and brine, dried ($MgSO_4$), and concentrated. Purification by flash chromatography on silica gel (7:3 hexanes/EtOAc) gave 12 mg (49%) of (−)-**4j** as a white solid. Prior to doping into liquid crystal hosts, the compound was recrystallized from absolute EtOH after filtration through a 0.45 μm PTFE filter: mp 77−80 °C; ^{1}H NMR (400 MHz, $CDCl_3$) δ 0.88 (t, J = 6.7 Hz, 6H), 1.26−1.50 (m, 68H), 1.78−1.89 (m, 4H), 1.99 (s, 6H), 2.03 (s, 6H), 4.05 (t, J = 6.5 Hz, 4H), 6.97 (d, J = 8.9 Hz, 4H), 7.33 (s, 2H), 8.08 (d, J = 8.9 Hz, 4H); ^{13}C NMR (100 MHz, $CDCl_3$) δ 14.1, 15.1, 20.4, 22.7, 26.0, 29.1, 29.4, 29.57, 29.61, 29.69, 31.9, 68.4, 114.5, 119.9, 123.6, 129.7, 132.7, 136.1, 140.0, 141.9, 143.4, 163.6, 164.1.

4-Hydroxy-2,2′,6,6′-tetramethyl-4′-[(4-(4-octyloxyphenyl)benzoyl)-oxy]-3,3′-dinitrobiphenyl (9). Under an Ar atmosphere, solid DCC (15 mg, 0.07 mmol) was added to a stirred solution of (±)-**8** (25 mg, 0.07 mmol), 4-octyloxy-4′-biphenylcarboxylic acid (24 mg, 0.07 mmol), and DMAP (9 mg, 0.07 mmol) in dry CH_2Cl_2 (5 mL). The mixture was stirred at room temperature for 24 h, filtered, and concentrated. The solid residue was redissolved in EtOAc, washed with 2 M aqueous HCl, H_2O, and brine, dried ($MgSO_4$), and concentrated. Purification by flash chromatography on silica gel (4:1 hexanes/EtOAc) gave 15 mg (32%) of racemic **9** as a white solid. The product was resolved by chiral stationary-phase HPLC (60:40 hexanes/EtOH, 4 mL/min); the first eluant was collected and concentrated to give **9** in optically pure form: mp 115−116 °C; ^{1}H NMR (400 MHz, $CDCl_3$) δ 0.89 (t, J = 6.8 Hz, 3H), 1.30−1.49 (m, 10H), 1.79−1.84 (m, 2H), 1.95 (s, 3H), 1.96 (s, 3H), 2.00 (s, 3H), 2.21 (s, 3H), 4.02 (t, J = 6.6 Hz, 2H), 7.00 (d, J = 8.8 Hz, 2H), 7.04 (s, 1H), 7.34 (s, 1H), 7.59 (d, J = 8.8 Hz, 2H), 7.70 (d, J = 8.6 Hz, 2H), 8.17 (d, J = 8.6 Hz, 2H), 10.05 (s, 1H); ^{13}C NMR (100 MHz, $CDCl_3$) δ 14.1, 15.2, 18.1, 20.4, 21.0, 22.7, 26.0, 29.2, 29.4, 31.8, 68.2, 115.0, 118.8, 123.4, 125.9, 126.8, 128.4, 130.1, 131.0, 131.4, 131.7, 134.0, 134.8, 137.0, 140.5, 141.7, 143.3, 145.3, 146.7, 154.1, 159.7, 163.9.

Anal. Calcd for $C_{37}H_{40}N_2O_8$: C, 69.36; H, 6.29; N, 4.37. Found: C, 68.90; H, 6.10; N, 3.92.

(−)-4-Decanoyloxy-2,2′,6,6′-tetramethyl-4′-[(4-(4-octyloxyphenyl)-benzoyl)oxy]-3,3′-dinitrobiphenyl ((−)-5). Under an Ar atmosphere, thionyl chloride (1.0 mL, 13 mmol) was added dropwise to a mixture of decanoic acid (3.5 mg, 0.02 mmol) and dry benzene (2 mL) at room temperature. After the mixture was refluxed for 2 h, it was concentrated to give decanoyl chloride as a colorless oil. Under an Ar atmosphere, a solution of optically pure **9** (10 mg, 0.02 mmol) and DMAP (2.5 mg, 0.02 mmol) in dry THF (3 mL) was added to the acid chloride. The mixture was stirred at room temperature overnight, diluted with EtOAc (20 mL), washed with 2 M aqueous HCl, H_2O, and brine, dried ($MgSO_4$), and concentrated. Purification by flash chromatography on silica gel (7:3 hexanes/EtOAc) gave 13 mg (99%) of (−)-**5** as a light brown solid: mp 81−82 °C; $[\alpha]_D$ −11.0 (*c* 0.3, $CHCl_3$); ^{1}H NMR (400 MHz, $CDCl_3$) δ 0.86−0.91 (m, 6H), 1.25−1.48 (m, 22H), 1.72−1.84 (m, 4H), 1.97 (s, 6H), 2.01 (s, 6H), 2.57 (t, J = 7.5 Hz, 2H), 4.02 (t, J = 6.6 Hz, 2H), 7.00 (d, J = 8.7 Hz, 2H), 7.15 (s, 1H), 7.35 (s, 1H), 7.59 (d, J = 8.7 Hz, 2H), 7.70 (d, J = 8.4 Hz, 2H), 8.17 (d, J = 8.4 Hz, 2H); ^{13}C NMR (100 MHz, $CDCl_3$) δ 14.1, 15.2, 20.4, 20.4, 22.7, 24.2, 24.6, 26.0, 28.8, 29.0, 29.2, 29.2, 29.4, 29.4, 31.8, 31.9, 34.0, 35.3, 68.2, 115.0, 123.5, 123.5, 125.9, 126.8, 128.4, 129.8, 131.0, 131.7, 136.3, 140.1, 141.7, 141.9, 143.3, 146.7, 159.7, 163.8, 171.1.

Anal. Calcd for $C_{47}H_{58}N_2O_9$: C, 71.01; H, 7.35; N, 3.52. Found: C, 71.14; H, 7.12; N, 3.37.

Ferroelectric Measurements. Texture analyses and transition temperature measurements for the doped liquid crystal mixtures were carried out using a Nikon Labophot-2 polarizing microscope fitted with a Instec HS1-i hot stage. Spontaneous polarization (P_S) values were measured as a function of temperature by the triangular wave method[30] (6 V/μm, 80−100 Hz) using a Displaytech APT-III polarization testbed in conjunction with the Instec hot stage. For each data point taken, the temperature of the sample was allowed to fully equilibrate in order to rule out any temperature effect during measurement. Polyimide-coated ITO glass cells (4 μm × 0.25 cm^2) supplied by Displaytech Inc. (Longmont, CO) were used for all the measurements. Good alignment was obtained by slow cooling of the filled cells from the isotropic phase via the N* and S_A* phases. Tilt angles (θ) were measured as a function of temperature between crossed polarizers as half the rotation between two extinction positions corresponding to opposite polarization orientations. The sign of P_S along the polar axis was assigned from the relative configuration of the electrical field and the switching position of the sample according to the established convention.[6]

S_C* Helical Pitch Measurements. Measurements of S_C* helical pitch were carried out at $T - T_C = -10$ K on a 150 μm film of the liquid crystal material in a planar alignment using a Nikon Labophot-2 polarizing microscope fitted with a Instec HS1-i hot stage. The helical pitch was measured as the distance between dark fringes caused by the periodicity of the S_C* helix.[31]

Calculations. All semiempirical calculations at the AM1 level were carried out using the Spartan 4.0 molecular modeling program.[32] Rotational energy profiles of the ester linking groups in the model systems 3-methyl-5-nitrophenyl benzoate and 3,5-dimethyl-2-nitrophenyl benzoate were obtained by constraining the torsional angle defined by C-6, C-1, O, and C(O) and by C-2, C-1, O, and C(O), respectively, and performing a full geometry optimization on the rest of the molecule. All minima were determined by full geometry optimization and confirmed as minima by vibrational analysis. Ab initio calculations of transverse dipole moments were carried out as single-point calculations on AM1-minimized structures with the HF/3-21G* basis set implemented in Gaussian 94.[33] The calculations were performed on a RISC-based IBM SP2 parallel processing computer.

Acknowledgment. We are grateful to the Natural Sciences and Engineering Research Council of Canada for support of this work. We also thank Profs. Mark Green, Mikhail Osipov, and David Walba for useful discussions.

JA990965M

(30) Miyasato, K.; Abe, S.; Takezoe, H.; Fukuda, A.; Kuze, E. *Jpn. J. Appl. Phys.* **1983**, *22*, L661.

(31) Martinot-Lagarde, P. *J. Phys.* **1976**, *C3*, 129.

(32) Wavefunctions, Inc., 18401 Von Karmann, #210, Irvine, CA.

(33) Gaussian 94, Rev. B.3: Frisch, M. J.; Trucks, G. W.; Schlegel, H. B.; Gill, P. M. W.; Johnson, B. G.; Robb, M. A.; Cheeseman, J. R.; Keith, T.; Petersson, G. A.; Montgomery, J. A.; Raghavachari, K.; Al-Laham, M. A.; Zakrzewski, V. G.; Ortiz, J. V.; Foresman, J. B.; Peng, C. Y.; Ayala, P. Y.; Chen, W.; Wong, M. W.; Andres, J. L.; Replogle, E. S.; Gomperts, R.; Martin, R. L.; Fox, D. J.; Binkley, J. S.; Defrees, D. J.; Baker, J.; Stewart, J. P.; Head-Gordon, M.; Gonzalez, C.; Pople, J. A. Gaussian, Inc., Pittsburgh, PA, 1995.